

# Ligand Control of Growth, Morphology, and Capping Structure of Colloidal CdSe Nanorods

Wei Wang,<sup>†,‡</sup> Sarbajit Banerjee,<sup>†,§</sup> Shengguo Jia,<sup>†,§</sup> Michael L. Steigerwald,<sup>†,‡</sup> and Irving P. Herman<sup>\*,†,§</sup>

Materials Research Science and Engineering Center, Department of Chemistry, and Department of Applied Physics and Applied Mathematics, Columbia University, New York, New York 10027

Received March 1, 2007

The organic capping ligands used in the colloidal synthesis of CdSe nanorods have a profound impact on nanorod shape, dimensions, and capping structure as is shown here by varying the length of the alkylphosphonic acid ligands used in synthesis. The shorter the ligand, the more elongated and branched are the resulting nanorods; when mixtures of alkylphosphonic acids are used, the higher the molar fraction of the shorter ligand, the more elongated and branched are the nanorods. <sup>31</sup>P and <sup>1</sup>H nuclear magnetic resonance (NMR) studies indicate that shorter ligands preferentially remain on the nanorod surfaces when mixtures of phosphonic acids are used during synthesis. Optical transmission spectroscopy shows decreased solubility of CdSe nanorods capped by relatively long ligands because of nanorod aggregation. The results suggest that substantial control of nanorod dimensions and properties can be achieved by selecting the appropriate ligands in the synthesis process.

## Introduction

Colloidal semiconductor nanostructures are receiving growing interest because of their promising optical, electrical, and magnetic properties. The ability to align and assemble nanorods may lead to applications such as light-emitting diodes, photovoltaic devices, and magnetic information storage.<sup>1–3</sup> To realize these applications, several challenges need to be met, such as controlling the size and shape of the nanocrystals, making the nanostructures well dispersed in certain solvents, and depositing them in a controlled manner.<sup>4</sup> Organic capping ligands have a profound effect on the growth mechanism and physical properties of colloidal nanocrystals and especially of nanorods. The capping ligands also influence solubility and can affect the effective volume of the nanocrystals, their surface charge, and their ability to adhere to substrates, which may affect the deposition of films of nanocrystals. For example, we have shown that the quality of CdSe nanocrystal films prepared by electrophoretic deposition is greatly influenced by the number of ligands on the nanocrystal surface.<sup>5</sup> Thus a detailed understanding about the functionality of the organic capping ligands is important for nanocrystal synthesis, properties, and applica-

tions, and this functionality is addressed here for CdSe nanorods.

Ab initio calculations have indicated that the relative binding energies of ligands to different facets affect the growth rates of the different facets and, consequently, control the geometry of the resulting nanoparticles.<sup>6</sup> Periodic density functional theory calculations have been employed to study the influence of ligand–surface interactions on the nanocrystalline growth of wurtzite CdSe and have indicated that the binding of the ligands is preferred at electron-poor sites relative to electron-rich surface sites.<sup>7</sup> Also, theoretical calculations aimed at elucidating the role of ligands in the anisotropic growth of CdSe nanocrystals have been performed using first principles modeling of unpassivated and surfactant-passivated bulk facets of wurtzite CdSe,<sup>8</sup> along with a detailed analysis of the structural reconstruction of the different surfaces.<sup>9</sup>

In other work, Searson and colleagues have shown that the growth rate and size of ZnO nanoparticles can be controlled by the injection of capping ligands, which adsorb onto the particle surface and provide a barrier to further growth.<sup>10</sup> Chaudret and his colleagues have reported that the aspect ratio of cobalt nanocrystals can be controlled by the alkyl chain length of the ligand.<sup>11</sup> Alivisatos and co-workers have reported the possibility of varying the diameter and

\* To whom correspondence should be addressed. E-mail: iph1@columbia.edu.

<sup>†</sup> Materials Research Science and Engineering Center.

<sup>‡</sup> Department of Chemistry.

<sup>§</sup> Department of Applied Physics and Applied Mathematics.

- (1) Hu, J. T.; Li, L. S.; Yang, W. D.; Manna, L.; Wang, L. W.; Alivisatos, A. P. *Science* **2001**, 292, 2060.
- (2) Huynh, W. U.; Dittmer, J. J.; Alivisatos, A. P. *Science* **2002**, 295, 2425.
- (3) Punties, V. F.; Krishnan, K. M.; Alivisatos, A. P. *Science* **2001**, 291, 2115.
- (4) Scher, E. C.; Manna, L.; Alivisatos, A. P. *Philos. Trans. R. Soc. London, Ser. A* **2003**, 361, 241.
- (5) Islam, M. A.; Xia, Y.; Telesca, D. A.; Steigerwald, M. L.; Herman, I. P. *Chem. Mater.* **2004**, 16, 49.

- (6) Puzder, A.; Williamson, A. J.; Zaitseva, N.; Galli, G.; Manna, L.; Alivisatos, A. P. *Nano Lett.* **2004**, 4, 2361.
- (7) Rempel, J. Y.; Trout, B. L.; Bawendi, M. G.; Jensen, K. F. *J. Phys. Chem. B* **2006**, 110, 18007.
- (8) Manna, L.; Wang, L. W.; Cingolani, R.; Alivisatos, A. P. *J. Phys. Chem. B* **2005**, 109, 6183.
- (9) Rabani, E. *J. Chem. Phys.* **2001**, 115, 1493.
- (10) Wong, E. M.; Hoertz, P. G.; Liang, C. J.; Shi, B. M.; Meyer, G. J.; Searson, P. C. *Langmuir* **2001**, 17, 8362.
- (11) Dumestre, F.; Chaudret, B.; Amiens, C.; Fromen, M. C.; Casanove, M. J.; Renaud, P.; Zurcher, P. *Angew. Chem., Int. Ed.* **2002**, 41, 4286.

aspect ratio of CdSe nanorods by using mixtures of HPA and TDPA.<sup>1</sup> Peng and collaborators observed that the synthesis of CdTe nanocrystals in non-coordinating solvents is strongly affected by the ligands and found the binding strength and steric factors of the ligands have a strong influence on the monomer activity (that is, the effective monomer concentration) and the morphology of the resulting nanocrystals.<sup>12</sup> Manna and his colleagues<sup>13</sup> found that the growth kinetics of colloidal CdTe nanorods can be dramatically influenced by the presence of impurities. By using very pure octadecylphosphonic acid (ODPA, 99%) during growth they synthesized approximately spherical nanocrystals, while when they used low-purity commercially available ODPA, they obtained nanorods or tetrapods. The active component that fosters branching and anisotropic growth may be a phosphonic acid with a short carbon chain present in commercially available ODPA.<sup>13</sup>

We choose CdSe nanorods as a model system to understand the role of ligands in the growth kinetics and morphology of one-dimensional nanostructures. Alivisatos, Peng, and colleagues have shown that CdSe nanorods with a desired shape and size can be synthesized using CdO as the Cd precursor.<sup>14–18</sup> Moreover, Peng and Peng<sup>17</sup> have systematically studied the nucleation and growth of colloidal CdSe nanorods for a variety of elongated shapes. They have investigated the influence of the initial Cd-to-Se precursor ratio, the monomer concentration, the reaction time, and the temperature of the growth system; they have also studied the growth kinetics via growth with multiple injections. Their results indicate that the shape evolution and growth kinetics of the elongated nanocrystals are consistent with a diffusion-controlled model; the size and shape of the resulting nanocrystals are mostly determined by the “magic-sized” nuclei and the concentrations of the monomers after the initial nucleation stage. This suggests that the ligand type may play a crucial role during the growth of colloidal CdSe nanorods, as further corroborated by periodic density functional theory calculations.<sup>7</sup> Even though dramatic progress has been made in synthesizing CdSe nanorods using colloidal chemistry,<sup>14–18</sup> no systematic study of the ligand functionality on the colloidal synthesis of CdSe nanorods has been reported to date.

In this paper, we have learned that the length of the ligands strongly affects the CdSe nanorod length and the possible occurrence of branching during growth. Also, we find that the properties of the resulting nanorods are influenced by the ligands used during growth.

## Experimental Section

**Chemicals.** CdO (99.99%), trioctylphosphine oxide (TOPO 99%), tributylphosphine (TBP), trioctylphosphine (TOP), meth-

ylphosphonic acid (MPA, 98%), dibutyl butylphosphonate (DBBP, 90%), and selenium powder were purchased from Aldrich. ODPA (97.1%), tetradecylphosphonic acid (TDPA, 98.8%), decylphosphonic acid (DPA, 98.6%), and hexylphosphonic acid (HPA, 99.9%) were purchased from Polycarbon Industries. ODPA and TDPA were purified by recrystallization in toluene before use. Diethyl 1-tetradecylphosphonate (DETDP, 98%) was purchased from Alfa Aesar. Chloroform-*d* (D, 99.8%) + 0.05% (v/v) tetramethylsilane (TMS) was purchased from Cambridge Isotope Laboratories. A Se-TBP stock solution (with 25% Se by mass) was prepared by mixing Se powder with TBP and then stirring for at least 24 h until the selenium was completely dissolved, giving an optically clear solution. This stock solution was prepared and stored in a glovebox under nitrogen.

**Characterization.** All <sup>31</sup>P and <sup>1</sup>H NMR analyses were recorded on a Bruker 300WB spectrometer. P(OCH<sub>3</sub>)<sub>3</sub> in C<sub>6</sub>D<sub>6</sub> (141 ppm) was used as an external standard for <sup>31</sup>P NMR. For transmission electron microscopy (TEM) imaging, the nanorods were deposited onto 400 mesh copper Formvar/carbon grids and analyzed using a JEOL 100 CX transmission electron microscope. The diameters, *D*, and lengths, *L*, of the rods were determined by measuring all the nanorods in a chosen area in the TEM image (>50 particles). The fraction of branched nanocrystals was determined by analyzing ~100 nanocrystals in a given area in the TEM image. All the TEM pictures were taken at 200 K magnification. The transmission of solutions of the nanorods was measured in a HP 8453 UV/visible spectrophotometer (Agilent) to determine the absorption peak of the first exciton of the nanorods and to analyze elastic scattering of aggregates of nanorods. All the UV–vis measurements were conducted within three days of synthesis unless otherwise specified.

**Synthesis.** CdSe nanorods were synthesized by a modification of the synthesis in ref 14. Unless otherwise specified, CdO (0.2054 g, 1.6 mmol), phosphonic acid ligands (3.2 mmol in total), and TOPO (with the total mass of TOPO and ligands fixed at 4.0 g) were loaded into the reaction flask (50 mL) and then heated to 300–320 °C under nitrogen flow until all the CdO reacted to give a transparent solution. This optically clear solution was heated to 320 °C and kept at this temperature for 10 min, and then it was cooled to room temperature under N<sub>2</sub> flow. After aging for at least 24 h, it was used directly without further purification.

In a nitrogen glovebox, Se-TBP (0.253 g with 25% Se by mass, 0.8 mmol of Se) was mixed with 1.447 g of TOP and 0.3 g of toluene to obtain the injection solution. This solution was then loaded into a 10 mL syringe and injected into the reaction flask at 320 °C. In all syntheses, the crystals were allowed to grow for 8 min at 300 °C, after which the heating mantle was removed and the reaction vessel was cooled to room temperature in the ambient environment. Chloroform (5 mL) was added into the flask at ~50 °C, and the entire solution was transferred to a 50 mL vial. Then methanol (10–15 mL) was added into the vial to precipitate the nanorods. The precipitated nanorods were separated by centrifugation and decantation and then redissolved in chloroform. CdSe nanorods were purified by reprecipitation with methanol and dissolved in chloroform again to obtain the “reprecipitated” CdSe nanorod solution.

To recover the nanorod capping ligands for NMR analysis, the reprecipitated CdSe nanorods were precipitated by adding methanol. The precipitate was isolated by centrifugation and decantation and then dried under nitrogen at 80 °C for at least 24 h. Subsequently, the nanorod powder was treated in aqua regia (1:3 concentrated HNO<sub>3</sub>/concentrated HCl). The digestion solution was extracted by ethyl ether, and this extract was washed with pure water three times. After evaporation of the ethyl ether, the white solid was character-

- (12) Yu, W. W.; Wang, Y. A.; Peng, X. *Chem. Mater.* **2003**, *15*, 4300.
- (13) Carbone, L.; Kudera, S.; Carlino, E.; Parak, W. J.; Giannini, C.; Cingolani, R.; Manna, L. *J. Am. Chem. Soc.* **2006**, *128*, 748.
- (14) Peng, X. G.; Manna, L.; Yang, W. D.; Wickham, J.; Scher, E. C.; Kadavanich, A.; Alivisatos, A. P. *Nature* **2000**, *404*, 59.
- (15) Manna, L.; Scher, E. C.; Alivisatos, A. P. *J. Am. Chem. Soc.* **2000**, *122*, 12700.
- (16) Peng, Z. A.; Peng, X. G. *J. Am. Chem. Soc.* **2001**, *123*, 1389.
- (17) Peng, Z. A.; Peng, X. G. *J. Am. Chem. Soc.* **2002**, *124*, 3343.
- (18) Peng, X. G. *Adv. Mater.* **2003**, *15*, 459.



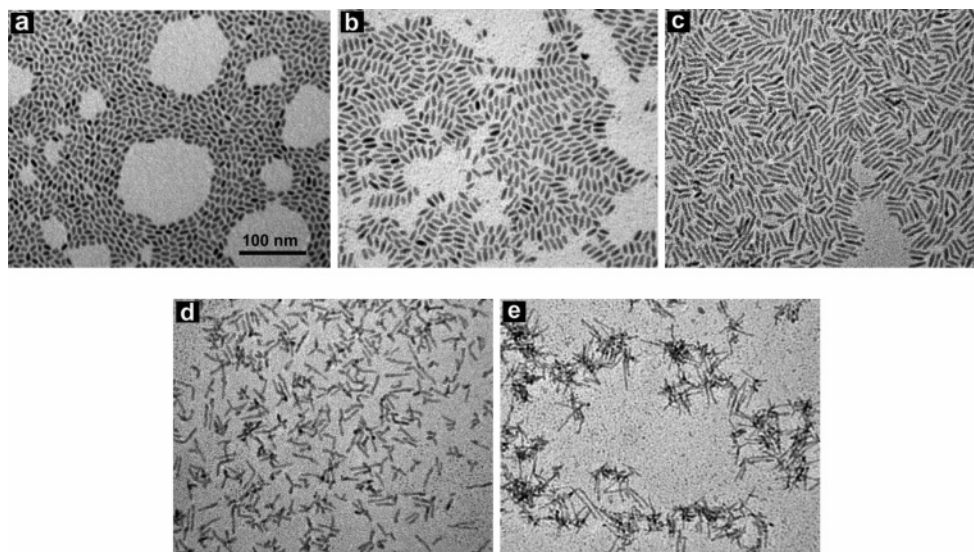


**Figure 1.** TEM images of CdSe nanorods synthesized using a single kind of ligand: (a) ODPA, (b) TDPA, (c) DPA, (d) OPA, and (e) HPA, as in Table 1. The scale is the same in each image.

**Table 1. Diameter ( $D$ ), Length ( $L$ ), and Aspect Ratio ( $L/D$ ) of the Nanorods Depicted in Figure 1, Synthesized Using Alkylphosphonic Acid Ligands with Different Alkyl Chain Lengths  $N^a$**

ligand	$N$	$D$ (nm)	$L$ (nm)	$L/D$	$f_{br}$	$\lambda_{abs}$ (nm)
ODPA	18	$3.8 \pm 0.5$	$9.5 \pm 1.1$	$2.5 \pm 0.6$	0%	626.0
TDPA	14	$4.1 \pm 0.6$	$14.3 \pm 1.6$	$3.5 \pm 0.9$	2%	630.9
DPA	10	$3.6 \pm 0.4$	$24.0 \pm 5.0$	$6.7 \pm 2.2$	8%	616.4
OPA	8	$3.4 \pm 0.4$	$34.5 \pm 7.0$	$10 \pm 4$	72%	613.9
HPA	6	$2.4 \pm 0.4$	$42.1 \pm 8.1$	$18 \pm 7$	>99%	597.9

<sup>a</sup> For each, the fraction of nanocrystals that are branched ( $f_{br}$ ) and the UV–vis absorption peak position ( $\lambda_{abs}$ ) of the nanorods are given. The listed uncertainties for the nanorod diameter, length, and aspect ratio are the measured  $1\sigma$  deviations.

ized by  $^{31}\text{P}$  and  $^1\text{H}$  NMR in chloroform- $d$  ( $\text{CDCl}_3$ ) at  $59^\circ\text{C}$ . In a control experiment, TDPA and TOPO were treated using the same procedure as the recovered ligands from the surface of the nanorods and then were characterized by  $^{31}\text{P}$  NMR.

## Results

**Effect of the Length of the Ligands on the Growth and Morphology of Colloidal CdSe Nanorods.** The results of syntheses performed by using ODPA, TDPA, DPA, OPA, and HPA as the ligand are summarized in Figure 1 and Table 1. The size, aspect ratio, and branching behavior of the resulting CdSe nanorods can be varied greatly by varying the length of the ligand used in the synthesis. A clear trend is that the shorter the phosphonic acid ligand, the more elongated are the resulting CdSe nanorods and the more likely is the formation of branched structures such as tetrapods.

The molar amounts of ligands (3.2 mmol), CdO (1.6 mmol), and Se precursor (0.8 mmol) and the total mass of phosphonic acids and TOPO (4.0 g) were kept the same in each synthesis. The variables were the alkyl chain length of the ligand tail and the molar amount of TOPO. The amount of TOPO varied from 7.58 mmol (when ODPA was used) to 8.97 mmol (when HPA was used, because the total masses of ligands and solvents were kept as constant). The length of the alkyl chain of the phosphonic acid ligands appeared to play a crucial role in determining the morphology of the

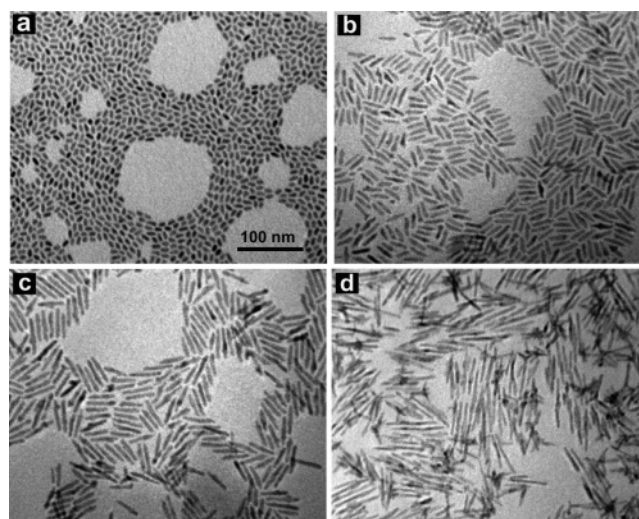


**Figure 2.** TEM images of CdSe nanorods synthesized using mixtures of ODPA and MPA with MPA molar fractions ( $f_{\text{MPA}}$ ): (a) 0, (b) 0.09, (c) 0.13, and (d) 0.25, as in Table 2. The scale is the same in each image.

resulting CdSe nanorods; we do not think the variation in the molar ratio of TOPO to Cd, 4.7–5.6, in these runs is important in affecting the morphology.

**Using Mixtures of Phosphonic Acids with Different Lengths.** CdSe nanorods with different lengths, aspect ratios, and degrees of branching were synthesized by using mixtures of ODPA and MPA. The results of the syntheses performed with MPA molar fractions,  $f_{\text{MPA}}$ , ranging from 0 to 0.25 are summarized in Figure 2 and Table 2. The higher the molar fraction of MPA, the more elongated and branched are the resulting nanorods. This is consistent with recent reports on the branched growth of CdTe by Manna et al.<sup>13</sup> when they added MPA to ODPA. When we increased the MPA molar fraction beyond 0.25 to 0.38, we were unable to obtain an optically clear Cd precursor.

Analogously, CdSe nanorods with different morphologies were synthesized by using mixtures of TDPA and HPA. The results of the syntheses performed with HPA molar fractions,  $f_{\text{HPA}}$ , ranging from 0 to 1 are summarized in Figure 3 and

**Table 2. Diameter (*D*), Length (*L*), and Aspect Ratio (*L/D*) of the Nanorods Depicted in Figure 2, Synthesized Using ODPa and MPA Ligands with the Molar Fraction  $f_{\text{MPA}} = ([\text{MPA}]/([\text{MPA}] + [\text{ODPA}]))^a$** 

$f_{\text{MPA}}$	<i>D</i> (nm)	<i>L</i> (nm)	<i>L/D</i>	$f_{\text{br}}$	$\lambda_{\text{abs}}$ (nm)
0	3.8 ± 0.5	9.5 ± 1.1	2.5 ± 0.6	0%	626.0
0.09	3.9 ± 0.6	26.0 ± 3.1	6.7 ± 1.9	<1%	634.5
0.13	4.1 ± 0.5	41.4 ± 5.2	10 ± 3	<1%	637.2
0.25	3.0 ± 0.4	64.1 ± 9.7	21 ± 7	26%	619.0

<sup>a</sup> For each, the fraction of nanocrystals that are branched ( $f_{\text{br}}$ ) and the UV–vis absorption peak position ( $\lambda_{\text{abs}}$ ) of the nanorods are given. The listed uncertainties for the nanorod diameter, length, and aspect ratio are the measured 1 $\sigma$  deviations.

Table 3. As the molar fraction of the HPA ligand increases, the nanorod length and branching fraction increases.

In addition, longer CdSe nanorods were grown when commercially available ODPa was used (see Supporting Information, Figure S1), while shorter nanorods were obtained (as shown in Figure 1a) when we used recrystallized ODPa. This points to the importance of purification.

When the phosphonic acid (TDPA) is substituted by the phosphonate ester (DETDP), the nanorods obtained are more elongated and branched. As seen for mixtures of phosphonic acids, mixtures of phosphonate esters also yield more elongated and branched nanorods. (Supporting Information shows TEM images of nanorods synthesized using DETDP and mixtures of DETDP and DBBP, Figures S2 and S3.)

#### Capping Structure of CdSe Nanorods. (a) <sup>31</sup>P and <sup>1</sup>H NMR of Ligands Present on the Surface of CdSe Nanorods.

<sup>1</sup>H NMR has previously been used to show that the predominant ligands recovered from the CdSe nanorod surface are the phosphonic acids that are used during the synthesis.<sup>12,17</sup> However, unambiguous and direct conclusions cannot be drawn by using only <sup>1</sup>H NMR because the H atoms in phosphonic acids, TOPO, phosphines, and so forth have similar chemical environments and their peaks overlap in the same spectrum. In contrast, there is only one P atom in each of these molecules, and the <sup>31</sup>P NMR peaks for trialkylphosphine oxides (~48 ppm), TBPSe (~37 ppm), Cd-TDPA (~25 ppm), and phosphonic acids (~38 ppm) are adequately separated.<sup>19,20</sup> Therefore, <sup>31</sup>P NMR was used to determine whether phosphonic acids or trialkylphosphine oxides are present in compounds recovered from the surface of the reprecipitated nanorods. Control experiments showed that neither trialkylphosphine oxides nor phosphonic acids are destroyed in the aqua regia used to digest the cores of the nanorods.

Figure 4a shows the <sup>31</sup>P NMR trace of the ligands recovered from reprecipitated CdSe nanorods synthesized using TDPA. There is a peak related to phosphonic acids and another peak corresponding to a Cd–phosphonic acid complex. (See Supporting Information Figure S4 and ref 20.) TOPO and TBPO <sup>31</sup>P NMR peaks are not seen, which indicates that TOP, TBP, TOPO, and TBPO may not be the primary capping ligands. (TOP and TBP can be oxidized to TOPO and TBPO in the digestion process.)

<sup>1</sup>H NMR is useful for identifying the length of the alkyl chain of the ligands. For CH<sub>3</sub>(CH<sub>2</sub>)<sub>*n*−1</sub>P(O)(OH)<sub>2</sub>, the chemical shift is approximately 0.8–1.0 ppm for protons in CH<sub>3</sub> and 1.1–1.9 ppm for the protons in (CH<sub>2</sub>)<sub>*n*−1</sub>. The number of the carbon atoms in the alkyl chain, *n*, can be determined by comparing the integrated peaks in these two areas, as shown in Figure 4b. <sup>1</sup>H NMR of the recovered substances from reprecipitated CdSe nanorods shows that the relative ratio of the areas of these two peaks is ~1:8, which is close to what is expected for TDPA (3:26). The recovered compounds may be TDPA and Cd-TDPA complexes. This confirms that the capping ligands present on the nanorod surfaces are mostly the phosphonic acids that are originally used in synthesis or their associated phosphonates.<sup>20</sup>

Figures 4c and 4d show the <sup>31</sup>P and <sup>1</sup>H NMR traces of the recovered compounds from reprecipitated CdSe nanorods synthesized using TDPA and HPA with a molar ratio of 1:1 ( $f_{\text{HPA}} = 0.5$ ). <sup>31</sup>P NMR shows the recovered compounds are phosphonic acids and their complexes. The molar ratio of TDPA and HPA on the nanorod surfaces was determined to be 1.6 from the ratio of the numbers of H atoms in CH<sub>3</sub> and CH<sub>2</sub> groups in the <sup>1</sup>H NMR traces. (Let us call this ratio of H atoms *z*. Say that the probability a ligand in this reaction mixture ends up on the nanorod surface is  $p_{\text{HPA}}$  for HPA and  $p_{\text{TDPA}}$  for TDPA, and the molar fractions of HPA and TDPA present on the nanorod surface are *x* and 1 − *x*. Then  $z = (10x + 26(1 - x))/(3x + 3(1 - x))$ . With  $z = 5.4$  from Figure 5d, then  $x = 0.61$ , and  $p_{\text{HPA}}/p_{\text{TDPA}} = 0.61/(1 - 0.61) = 1.6$ .) Even after taking into account experimental uncertainties, it is clear that there is more HPA than TDPA on the nanorod surface even though equal molar amounts were used during synthesis.

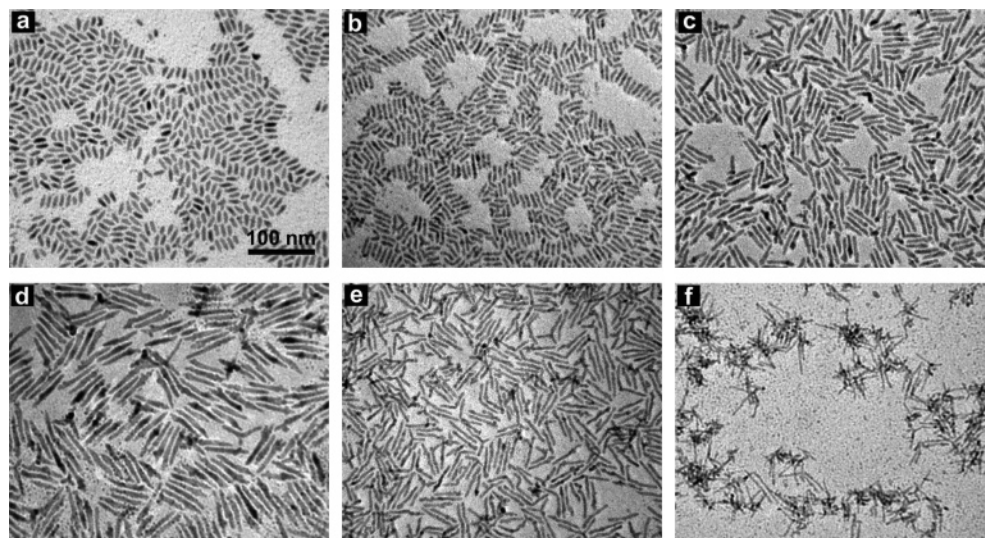
(b) *Floating Aggregates in the Nanorod Solutions.* The optical transmission spectra of the CdSe nanorods in Figure 5 show that the first exciton absorption peak varies from 590 to 650 nm, depending on the nanorod dimensions. The spectra have been measured for nanorods cleaned by multiple reprecipitation cycles with methanol. The axis labeled as “absorbance” actually includes decreased transmittance due to absorption and elastic light scattering. There is no detectable light scattering at long wavelengths (700–850 nm) when the nanorods are dispersed well in chloroform. In contrast, light scattering is observed at these longer wavelengths when the concentration of nanorod aggregates in the solution is sufficiently high. Aggregation will increase the total scattering rate by roughly the number of particles in the aggregate if all the aggregate dimensions are much smaller than the wavelength.<sup>21</sup> This is used as a measure of the nanorod solubility.

Figure 5a shows there is no detectable light scattering at longer wavelengths for CdSe nanorods synthesized using DPA, OPA, or HPA, which suggests that these nanorods are well dispersed in chloroform. (After 1 week, precipitates are seen on the bottom of the glass vial, which are presumably very large aggregates, but light scattering at longer wavelengths is not seen during this week.) In contrast, an increased baseline due to light scattering is seen at longer wavelengths for freshly prepared nanorods synthesized using ODPa or

(19) These data are obtained at 59 °C on the same Bruker 300WB spectrometer, using chloroform-*d* as the solvent.

(20) Liu, H. T.; Owen, J. S.; Alivisatos, A. P. *J. Am. Chem. Soc.* **2006**, *129*, 305.





**Figure 3.** TEM images of CdSe nanorods synthesized using mixtures of TDPA and HPA with HPA molar fractions ( $f_{\text{HPA}}$ ): (a) 0, (b) 0.12, (c) 0.25, (d) 0.38, (e) 0.50, and (f) 1.00, as in Table 3. The scale is the same in each image.

**Table 3. Diameter ( $D$ ), Length ( $L$ ), and Aspect Ratio ( $L/D$ ) of the Nanorods Depicted in Figure 3, Synthesized Using TDPA and HPA Ligands with the Molar Fraction  $f_{\text{HPA}}$  ( $[\text{HPA}]/([\text{HPA}] + [\text{TDPA}])$ )<sup>a</sup>**

$f_{\text{HPA}}$	$D$ (nm)	$L$ (nm)	$L/D$	$f_{\text{br}}$	$\lambda_{\text{abs}}$ (nm)
0	$4.1 \pm 0.6$	$14.3 \pm 1.6$	$3.5 \pm 0.9$	2%	630.9
0.12	$3.3 \pm 0.4$	$23.7 \pm 3.7$	$7.2 \pm 2.0$	12%	615.1
0.25	$3.7 \pm 0.5$	$36.0 \pm 5.8$	$9.7 \pm 2.9$	14%	622.8
0.38	$4.2 \pm 0.4$	$59.8 \pm 7.0$	$14 \pm 3$	9%	643.3
0.50	$3.1 \pm 0.3$	$44.6 \pm 7.1$	$14 \pm 4$	49%	611.0
1.0	$2.4 \pm 0.4$	$42.1 \pm 8.1$	$18 \pm 7$	>99%	597.9

<sup>a</sup> For each, the fraction of nanocrystals that are branched ( $f_{\text{br}}$ ) and the UV-vis absorption peak position ( $\lambda_{\text{abs}}$ ) of the nanorods are given. The listed uncertainties for the nanorod diameter, length, and aspect ratio are the measured  $1\sigma$  deviations.

TDPA, indicating the formation of nanorod aggregates (that are still small enough to remain dispersed). Figure 5b shows that there is a significant contribution from light scattering at longer wavelengths for CdSe nanorods synthesized using only ODPA or mixtures of MPA and ODPA, while no detectable light scattering is seen for CdSe nanorods synthesized using mixtures of ODPA and HPA. Figure 5c shows that CdSe nanorods synthesized using mixtures of TDPA and HPA are better dispersed in chloroform than those synthesized using only TDPA. Figure 5d shows that when DETDP is used (which has the same alkyl chain as TDPA but a different terminal functional group), the nanorods dissolve very well and no scattering is observed at longer wavelengths. These nanorods remain well dispersed in chloroform for more than 10 months. The solubility trends observed are reproducible from batch to batch; nanorods

synthesized using shorter chain ligands or mixtures of long and short chain ligands exhibit greater solubility and yield more stable solutions as compared to nanorods synthesized using longer chain phosphonic acids.

#### Effects of Quantum Confinement in CdSe Nanorods.

The exciton absorption peak of these CdSe nanorods demonstrates quantum confinement. The exciton peak energy is plotted as a function of  $(2.33/D^2 + 1/L^2)$  in Figure 6 for all the nanorods capped by phosphonic acids (that are produced in syntheses yielding a branching fraction smaller than 15%). A linear fit is expected for isotropic carriers in a cylindrical rod of diameter  $D$  and length  $L$  of constant potential that is embedded in an infinite potential.<sup>22</sup> All these data can be linearly fit fairly well with a carrier mass of  $0.146 m_e$  (with  $m_e$  being the mass of a free electron), which represents the reduced mass of the effective masses of electrons and holes. (This value is reasonable given the approximations in the model, and the effective masses of electrons, perpendicular band holes, and parallel band holes of  $0.13 m_e$ ,  $0.45 m_e$ , and  $1.1 m_e$ , respectively, in bulk CdSe.<sup>23</sup>) This fit is largely insensitive to  $L$ .

## Discussion

**Effect of the Length of the Ligands, Mixtures of Ligands, and the Ligand Binding Group on the Growth and Morphology of Colloidal CdSe Nanorods.** This synthesis involves two steps. In the first step of the reaction, the alkylphosphonic acids react with CdO to form Cd-phosphonic acid complexes. In the second step, these complexes react at the injected temperature (320 °C), forming various nuclei or exceptionally stable clusters by reacting with the injected Se precursor.<sup>16,17,24</sup> The complexes with longer chain ligands are more stable,<sup>24</sup> and thus the active species are generated relatively slowly. In contrast, com-

(21) This is based on the analytic solution for the total elastic scattering cross section for spheres of diameter  $D$  ( $\ll \lambda$ , the wavelength), which varies as  $D^6$  and of cylinders of diameter  $D$  ( $\ll \lambda$ ) and length  $L$  ( $> \lambda$ ), which varies as  $D^4 L$ . (van de Hulst, H. C. *Light Scattering by Small Particles*; Dover: New York, 1981.) We can assume that the general dependence of the cross section for a cylinder is  $D^4 L^q$ , where  $q \rightarrow 2$  as  $L \rightarrow D$  ( $\ll \lambda$ ) and  $q \rightarrow 1$  for  $L \gg D$  and longer than  $\lambda$ . When  $M$  identical spheres aggregate to form an identical larger sphere of radius  $M^{1/3}D$  ( $\ll \lambda$ ), the elastic scattering rate increases as  $M$ . When  $M$  identical cylinders aggregate together laterally to form identical cylinders of diameter  $M^{1/2}D$  ( $\ll \lambda$ ) and the same length  $L$ , the scattering rate increases as  $M$ . When these  $M$  cylinders instead aggregate by lining up end-to-end (which is less likely), the scattering rate increases as  $M^{q-1}$ , where  $1 \leq q \leq 2$ .

(22) Liboff, R. L. *Introductory quantum mechanics*, 4th ed.; Addison-Wesley: San Francisco, CA, 2003.

(23) Gaponenko, S. V. *Optical properties of semiconductor nanocrystals*; Cambridge University Press: New York, 1998.

(24) Kim, J. I.; Lee, J. K. *Adv. Funct. Mater.* **2006**, *16*, 2077.

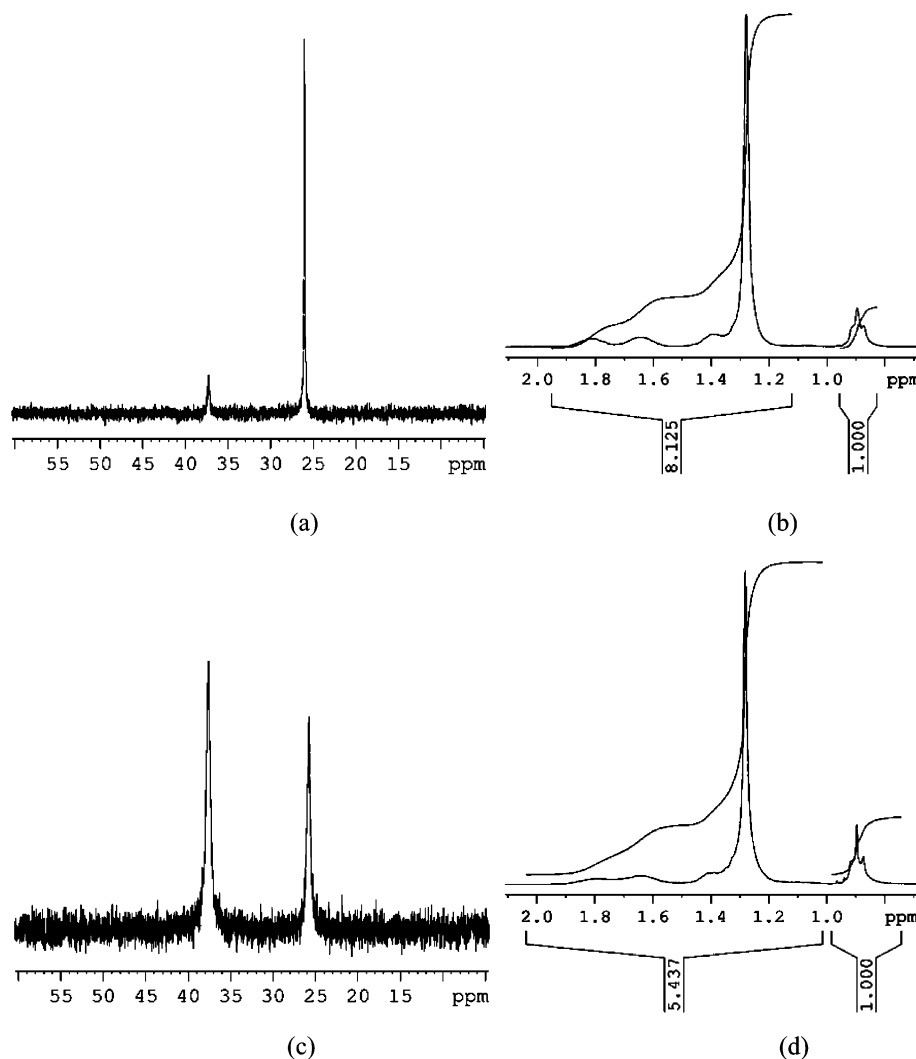


**Figure 4.** (a and b)  $^{31}\text{P}$  NMR and  $^1\text{H}$  NMR traces of the compounds recovered from purified CdSe nanorods synthesized using TDPA; (c and d)  $^{31}\text{P}$  NMR and  $^1\text{H}$  NMR traces of the compounds recovered from purified CdSe nanorods synthesized using TDPA and HPA with a molar ratio of 1:1.

plexes with shorter chain ligands react more rapidly, leading to a higher concentration of nuclei upon reaction with the Se precursor. Because higher monomer concentration favors anisotropic growth, according to the diffusion model,<sup>16</sup> precursors with shorter ligands tend to induce more anisotropic growth. The intrinsic anisotropy of the wurtzite structure therefore leads to preferential growth along the *c*-axis and the resulting formation of nanorods.

Moreover, monomers bound by shorter chain ligands are more mobile and reactive than are their longer chain counterparts, because they are less sterically hindered. This leads to faster diffusion of the nuclei and a higher growth rate. Thus, for shorter chain ligands, the monomer concentration, diffusion speed, and reactivity of the monomers are higher; consequently, anisotropic growth is favored. The most anisotropic growth observed here occurs when HPA is used. Branching is seen due to stacking faults/twinning defects in the nuclei.<sup>13</sup> Because precursors with a shorter chain lead to a higher concentration, mobility, and reactivity of the monomers and thus exhibit faster growth, the nanorods synthesized by using HPA are more susceptible to such defects and thus show extensive branching.

CdSe nanorods synthesized using mixtures of phosphonic acids with different lengths tend to grow longer with increased anisotropy (compared to using only long chain phosphonic acids: ODPA or TDPA) because of the role played by the shorter chain ligands (MPA or HPA) in both nucleation and growth. We expect that nanorods with a desired length and degree of branching can be obtained by using mixtures of phosphonic acid ligands with the proper molar ratio.

Notably, the phenomenon observed here is likely to be primarily a kinetic effect, because the binding energies of ligands with different chain lengths are not expected to be very different. Previous calculations have been focused on the stabilization of different facets in terms of surface energy considerations.<sup>6–9</sup> There has not been much work devoted to studying the effect of the ligand chain length on the kinetics of this high-temperature process. Alivisatos and colleagues have pointed out the longer phosphonic acid chains result in slower growth of the nanorods because of steric hindrance of the longer chain.<sup>4</sup> Work by Peng and co-workers also suggested the steric effects of the ligands can dramatically affect the activity coefficients of the mono-

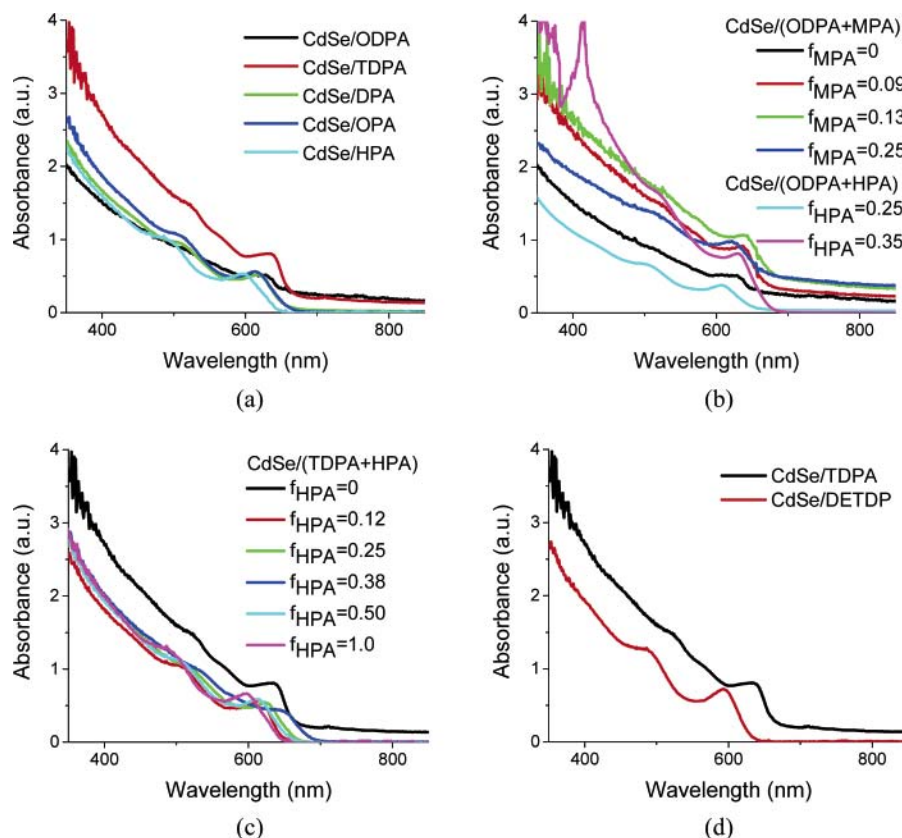


**Figure 5.** UV-vis absorption spectra of chloroform solutions of CdSe nanorods synthesized using (a) ODPA, TDPA, DPA, OPA, and HPA; (b) mixtures of ODPA and MPA with MPA molar fractions of 0, 0.09, 0.13, and 0.25 and using ODPA and HPA, with HPA molar fractions of 0.25 and 0.35; (c) mixtures of TDPA and HPA with HPA molar fractions of 0, 0.12, 0.25, 0.38, 0.50, and 1.0; (d) using TDPA and DETDP.

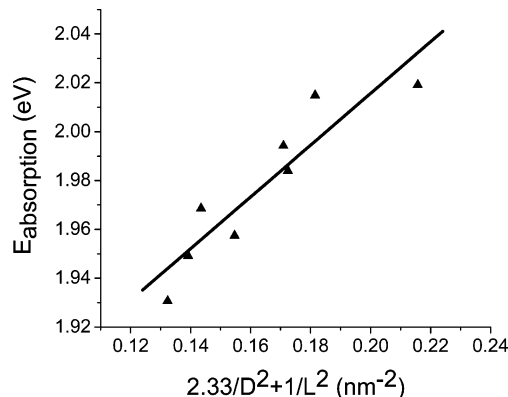


**Figure 6.** Plot of the energy of the first exciton absorption peak as a function of  $(2.33/D^2 + 1/L^2)$ . CdSe nanorods (with a branching fraction <15%) from all synthesis runs are included. The line has a slope of 1.06 eV·nm<sup>2</sup> and a y intercept of 1.80 eV. The *R* value of the fit is 0.92.

mers.<sup>12</sup> A detailed modeling of the kinetics of this process is beyond the scope of this paper.

Commercially available ODPA may include short chain ligands, such as ethylphosphonic acid,<sup>13</sup> which can facilitate the elongated growth of nanorods and branched nanocrystals. This explains why long CdSe nanorods were grown when commercially available ODPA was used, while short nanorods were obtained when we used recrystallized ODPA.

The nanorods synthesized by using DETDP are more elongated and branched than those synthesized by using TDPA. These nanorods are attractive because they provide a very stable solution in chloroform and have a high solubility in most nonpolar solvents. The structure of the

precursor complex formed with CdO when DETDP is used as a ligand has not yet been determined.

**Nature of the Capping Structure.** When CdSe nanorods are synthesized using mixtures of two phosphonic acid ligands with different alkyl chain lengths, both ligands are present on the surface, but there is more (by mole) of the shorter length ligand than the longer one. This is seen for CdSe/(TDPA + HPA) nanorods by using NMR.

The Cd precursor used during synthesis, such as the Cd-TDPA or Cd-ODPA complex, is present in excess, and after reaction some of it might remain on the nanorods. The polar solvents used in the precipitation process can precipitate this complex, and thus reprecipitated nanorods may be contaminated by this species. It is possible that this species is a cross-linked polymer of Cd and phosphonic acid. The remnant cross-linked Cd gels may significantly affect the solubility of the nanorods by trapping them in some sort of a network. The observed variability in solubility could be due to the different degrees of polymerization obtained with the different ligand molecules. Shorter chain phosphonic acid gels are expected to have a higher solubility, and thus nanorods prepared using shorter-chain ligands may be contaminated with less of the Cd-containing polymer, thereby leading to greater solubility for these nanorods. Another possibility is that ligand molecules may be trapped within the ligand shell due to van der Waals interactions between the alkyl chains of the ligands. Hydrogen bonding interactions between trapped ligands may lead to the aggregation of the nanorods. The binding group and alkyl chain likely influence the degree of polymerization and the number of excess ligands trapped

on the nanorod surfaces, but the interplay of these factors is still not well understood.

### Conclusions

The length of the organic capping ligand has a profound effect on the growth kinetics of colloidal CdSe nanorods and the stability of the nanorod solution. Clear trends are as follows: the shorter the alkylphosphonic acid ligand, the more elongated the resulting nanorods and the more the branching, and when mixtures of alkylphosphonic acids are used, the higher the molar fraction of the shorter ligand, the more elongated and branched are the nanorods. The capping ligands on these nanorods are phosphonic acids, and when phosphonic acid mixtures are used, the shorter ligands selectively remain on the inorganic surface. This work demonstrates the possibility of systematically tuning the morphology and properties of CdSe quantum dots by modifying the ligands used in synthesis.

**Acknowledgment.** This work is financially supported primarily by the MRSEC program of the National Science Foundation under Award No. DMR-0213574 and partially by the New York State Office of Science, Technology, and Academic Research (NYSTAR) and the NSEC program of the National Science Foundation under Award No. CHE-0641523. The authors thank Louis Brus for the use of his synthesis facilities and Haitao Liu for discussions and for making a copy of ref 20 available before publication.

**Supporting Information Available:** TEM images of CdSe nanorods synthesized using ODPa (commercially available), DETDP, and mixtures of DETDP and DBBP, and  $^{31}\text{P}$  NMR traces of the optically clear Cd precursor (when TDPA was used as the ligand) and TOPO in chloroform (reference sample), at 59 °C, are available (PDF). This material is available free of charge via the Internet at <http://pubs.acs.org>.

CM0705791